

Study of the Consequences of the Front External Reflection on the Electric Parameters of a Thin Film Cu (In,Ga) Se₂ Solar Cell

Alain Kassine Ehemba^{*}, Ibrahima Wade, Mouhamadou M. Soce, Djimba Niane and Moustapha Dieng

Laboratory of Semiconductors and Solar Energy, Faculty of Science and Technology, Cheikh Anta Diop University of Dakar, Dakar, Senegal
ehembaalain@yahoo.fr

Available online at: www.isca.in, www.isca.me

Received 20th September 2016, revised 3rd October 2016, accepted 23rd October 2016

Abstract

We study in this paper the effect of the front external reflection of incidental photons on the electric parameters such as the open circuit voltage V_{oc} , the short circuit current density J_{sc} , the maximum power P_m of the cell and external quantum efficiency EQE. The optimization of these parameters makes it possible to improve the performances of the solar cell of type n-ZnO/n-CdS/p-Cu (In, Ga) Se₂. We use a broad range of reflection going from 0%, use of ideal anti-reflecting layer, to a reflection of 80% which corresponds to a very weak absorption. We note that with the use of an "ideal" anti-reflecting layer, we obtained a short circuit current density of $0.0325\text{mA}\cdot\text{cm}^{-2}$, an open circuit voltage of 0,8337V, a maximum power of cell of 0.0233mW and a maximum value of the external quantum efficiency of 99.29%. However these physical parameters are deeply affected by the external front reflection. All the physical parameters studied decrease considerably. We find for a front reflection of 80%, a short circuit current density of $0.0065\text{mA}\cdot\text{cm}^{-2}$, an open circuit voltage of 0,7923V, a maximum power of cell of 0.0045mW and a maximum value of the external quantum efficiency of 19.86%.

Keywords: Front external reflection, Cu (In,Ga) Se₂, PC1D, electric parameters, EQE, IQE.

Introduction

The performances of a silicon or thin film solar cell depend not only on the internal parameters of the cell but also of the external use parameters of use of the cell. Our studies were initially based on the improvement of the performances of the cell by optimizing its internal parameters such as the donors doping density, the acceptors defects, the atomic ratios of concentrations of the base, and others^{1,4}. Then we were interested in optimization of the external parameters of use of the solar cell such as the temperature of use^{5,6}. The losses by reflection can be related to two principal parameters: i. The internal factors of which mainly the refractive index of the material which is equal to 3.45 in this study. That is to say approximately 30% of the incidental light is considered. ii. The external factors which can either attenuate this reflection by the use of anti-reflecting layer, or to increase this reflection by decreasing the absorption of the incidental light beam (case of dust).

We study the effect of the external front. However we use a broad range of reflection coefficients going from 0% to 80% to take into account all these parameters. We study the impact of the front external reflection on the electric parameters such as the short circuit current density J_{sc} , the open circuit voltage V_{oc} , the maximum power of the cell P_m and the external quantum efficiency EQE. The optimization of these parameters makes it possible to improve the performances of the cell. The study is based on a cell of n-ZnO/n-CdS/p-CIGS type as Figure-1 indicates it.

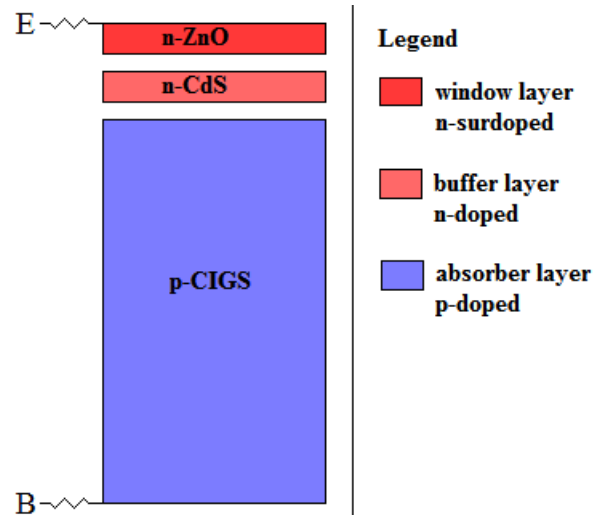


Figure-1
Device schematic

Materials and Methods

In the bibliography, front external reflection studies were carried out but they were based more particularly on the properties of material used like anti-reflecting layer such as ZnO, or on the metal contacts which can play a role of reflectors^{7,8}. This front reflection can indeed be due to intrinsic natural factors with materials or to external factors. All these factors contribute to the increase of the reflection decreasing consequently the absorption of the incidental photons.

Our study will relate not on the causes of the front external reflection but to their effects on the electric parameters of the cell. The reflection coefficients vary from 0% to 80%, a range of relatively large value to take into account all the factors that are likely to increase the reflection. However they carried out works concern three phases.

The first phase of our studies relate to the handling of the fundamental equations which govern the operation of a cell and utilizing the optical effects. These equations leave the equation of Poisson, the equations of continuity and the transport equations. We had to develop these equations before⁹.

The relation 1 shows the Poisson's equation with ϵ_s the dielectric permittivity of the semiconductor and the density of

$$\text{space charge } \rho: \nabla^2 V = -\frac{\rho}{\epsilon_s} \quad (1)$$

The relations 2 and 3 give the equations of continuity.

$$\text{For electrons } \frac{\partial n}{\partial t} = \frac{1}{e} \text{div} \vec{J}_n + G_n - R_n \quad (2)$$

$$\text{For holes } \frac{\partial p}{\partial t} = -\frac{1}{e} \text{div} \vec{J}_p + G_p - R_p \quad (3)$$

With: \vec{j}_n and \vec{j}_p densities of current of the electrons and the holes respectively, G_n and G_p rates of generations of the electrons and the holes respectively, R_n and R_p rates of recombination of the electrons and the holes respectively, e is the elementary electric charge.

The Relations 4 and 5 present the transport equations.

$$\vec{J}_p = -eD_p \vec{\nabla} p - ep\mu_p \vec{\nabla} V + p\mu_p kT \vec{\nabla} (n_i L_n) \quad (4)$$

$$\vec{J}_n = eD_n \vec{\nabla} n - en\mu_n \vec{\nabla} V - n\mu_n kT \vec{\nabla} (n_i L_n) \quad (5)$$

The second stage consists with the simulation of a solar cell of n-ZnO/n-CdS/p-CIGS type using the PC1D5. It is a quasi one-dimensional program conceived to simulate solar cells and able to solve the nonlinear coupled equations which control the physical phenomena of the studied device. It is software developed at the University South Wales of Sydney in Australia and distributed by Photovoltaics Special Research Center. The PC1D makes it possible to approach complex studies such as the strong rates of doping, raised levels of injection, the no plane structures and the transients^{10,11}.

However it is software used especially for the crystal structures in particular containing Silicon. We adapted it to the cells containing Cu (In,Ga) Se₂ thin film. The Table-1 presents the properties of materials used for simulation.

Table-1
Physical properties of materials

	n-ZnO	n-CdS	P-Cu(In,Ga)Se ₂
Thickness (μm)	0.05	0.05	2.5
Dielectric constant	10	13.6	13.6
Band gap (eV)	3.3	2.4	1.2
Intrinsic. Conc. At 300K (cm ⁻³)	1.99×10 ⁻⁹	0.04353	5.232×10 ⁸
Refractive index	3.45	3.45	3.45

The third part of the work concerns the tracing of the curves using Matlab. It is visualization and computation software, whose basic entities are matrices. MATLAB is an abbreviation of Matrix Laboratory. It is a language interpreted which proposes facilities of programming and visualization, as well as a great number of functions carrying out various numerical methods^{12,13}.

The Figure-2 presents the energy bands of the window layer, the buffer layer and the absorber layer.

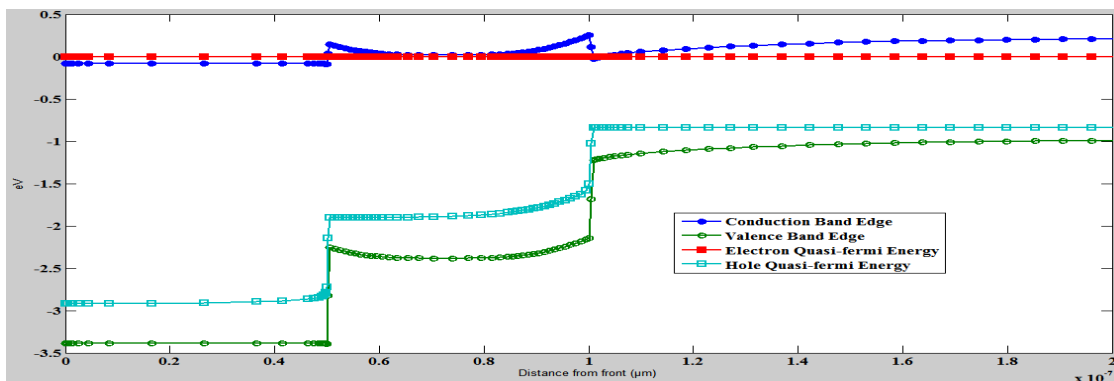


Figure-2
Energy bands

However the cut with at the back field was made at a depth of $0.1\mu\text{m}$ in the absorber layer for better perceiving the hetero junctions ZnO/CdS and CdS/Cu(In,Ga)Se_2 . From $0\mu\text{m}$ to $0.05\mu\text{m}$ we are in the ZnO window layer doped N^+ with a broad gap of 3.3eV . This high gap explains the distance which separates the conduction and valence bands. From $0.05\mu\text{m}$ to $0.1\mu\text{m}$ we approach the CdS buffer layer which is doped N . The noted slope is due on the one hand to the formation of the ZnO/CdS hetero junction because the electrons quasi-Fermi energy of materials must correspond. In addition we note the weaker gap of CdS which is of 2.4eV which explains also the proximity of the conduction and valence bands edge. From $0.1\mu\text{m}$ to $0.2\mu\text{m}$ we are in the absorbing layer of the cell which is a Cu(In,Ga)Se_2 thin film doped p . Its gap weaker 1.2eV and the correspondences of the quasi-Fermi energies explain the second slope. The tunnel effects at the hetero junctions, which can be a trap for the minority carriers, are not taken into account.

The three combined stages of our work enable us to advance with logic towards obtaining right and reliable results. Thus we studied the effect of the reflection on the short circuit current density J_{sc} , the open circuit voltage V_{oc} , the maximum power P_m of the cell and the variation of the external quantum efficiency EQE . We take into account a broad band of the irradiation, which contains wavelengths from 300nm to 1200nm , with a constant incidental illumination of 0.1W.cm^{-2} , under standard condition AM1.5 .

Results and Discussion

Consequences of the front external reflection on the short circuit current density J_{sc} : The short circuit current density J_{sc} expressed in mA.cm^{-2} is the current density which circulates in the cell under illumination and without delivered voltage. Indeed for a real cell J_{sc} is translated by the relation:

$$J_{sc} = J_{ph} - J_s \left[e^{\frac{qV}{kT}} - 1 \right] \quad (6)$$

The Figure-3 presents the variation of the short circuit current density of the cell according to the front external reflection.

The photovoltaic solar cell functions in rectifying device. It explains the negative sign of the current density. For a front reflection null we note a short circuit current density $|J_{sc}|$ equal to 0.0325mA.cm^{-2} . This value decreases with the increase in the front external reflection to be equal to 0.0065mA.cm^{-2} with a reflection of 80% . This phenomenon is explained by the proportionality of the short circuit current density with the incidental luminous flux. More the reflection of this incidental flux is significant less the photocurrent density is significant.

Consequences of the front external reflection on the open circuit voltage V_{oc} : The fundamental equation of the voltage V delivered by a photovoltaic cell at the boundaries of its circuit of use is given by:

$$V = \left(\frac{kT}{q} \right) \log \left(1 + \frac{J_{ph} - J}{J_s} \right) - R_s J \quad (7)$$

We note that J_{ph} is the photocurrent density, J_s the saturation current density, J the current density at the boundaries of the circuit of use and R_s series resistance.

The open circuit voltage V_{oc} expressed in Volt is the voltage which reigns in the cell when no current circulates there ($J=0$). Indeed the V_{oc} is evaluated while applying:

$$V_{oc} = \left(\frac{kT}{q} \right) \log \left(1 + \frac{J_{sc}}{J_s} \right) \quad (8)$$

The Figure-4 gives the variation of the open circuit voltage according to front external reflection.

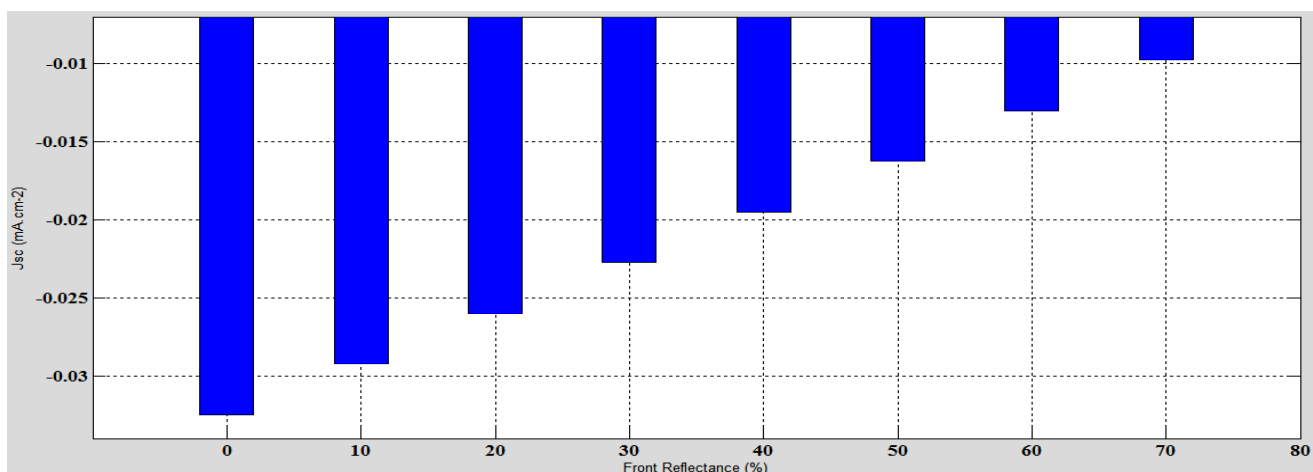


Figure-3
 Variation of the short circuit current density J_{sc} according to the front external reflection front

For an easier reading of the found results, we use the bar diagrams. The front external reflection varies from 0 to 80% of incidental luminous flux. When a reflection does not intervene we note a maximum open circuit voltage of 0.8337V. When this reflection increases the open circuit voltage decreases. We obtain for a reflection of 80%, a minimal voltage of 0.7923V. This behavior of the Voc is due to the fact that the short circuit current density Jsc is proportional to incidental luminous flux. The increase of the reflection contributes to the reduction of the absorbed flux, which causes the drop of the open circuit voltage Voc.

Consequences of the front external reflection on the maximum power Pm of the solar cell: The power of a solar cell of 1cm² can be evaluated by applying the relation:

$$P = J \times V \tag{9}$$

We can then evaluate a maximum power which corresponds to the product of maximum voltage Vm and the maximum current density Jm:

$$P_m = J_m \times V_m \tag{10}$$

The Figure-5 presents the variation of this maximum power according to the front external reflection.

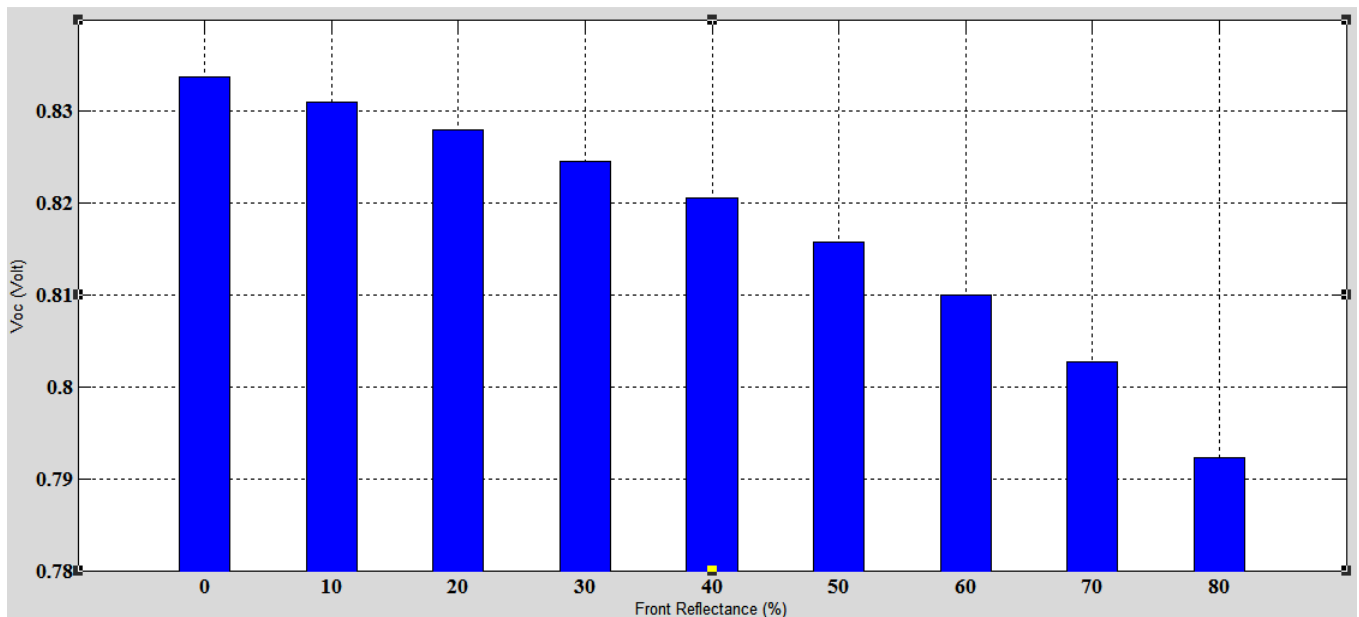


Figure-4
 Variation of the open circuit voltage Voc according to the front external reflection

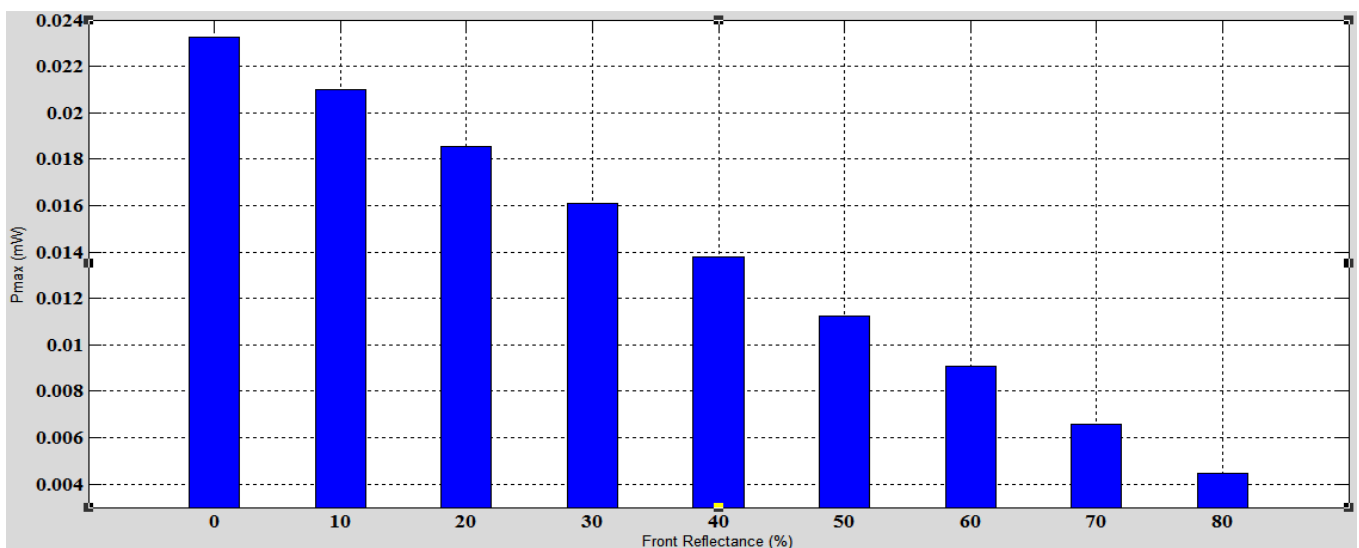


Figure-5
 Variation of the maximum power Pm of the cell according to the front external reflection

For a null reflection there is a maximum power of 0.0223mW. This power of the cell decreases with the increase in the reflection coefficient to equalize a minimal value of 0.0045mW for a front external reflection of 80%. The behaviors of the open circuit voltage and the short circuit current density with the increase in the coefficient of reflection make it possible to predict and explain the fall of the maximum power of the device.

Consequences of the front external reflection on the quantum efficiency: The quantum efficiency of the solar cell is the ratio of the number of collected charges and the number of incidental photons. We study in this work the two types of quantum efficiency. The internal quantum efficiency IQE which is the ratio of the number of collected charges and the number of photons really absorbed. It corresponds to the front reflection null (R=0). The characterization of the cell by its quantum efficiency makes it possible to do without the studies of transmittance and reflectance. The external quantum efficiency EQE which is the ratio of the number of collected charges and the number of incidental photons. It corresponds to the other reflection coefficients different from 0.

The Figure-6 presents to us the IQE and the variation of the EQE according to the front external reflection.

For incidental wavelengths going from 300nm to 1200nm we note, however the value of the front external reflection, a broad range of absorption. In the same way however the reflection, the quantum efficiency is the coefficient is cancelled for an incidental wavelength of 960nm. This value corresponds to an incidental energy of approximately 2.4eV. This energy is in agreement with the gap of the CdS buffer layer used which is

also 2.4eV. However the impact of the front external reflection consists in the reduction of external quantum efficiency. For better determining this reduction we interpret the indications of Table-2. The maximum value of external quantum efficiency drops considerably with the increase of the front reflection. It passes from 99.29% for a null coefficient of reflection to 19.86% for a coefficient of reflection equal to 80%. This reduction is physically explained by the fact that quantum efficiency is related to the spectral sensitivity. Indeed when the front reflection increases, the spectral response of the cell decreases owing to the fact that the current produced compared to the received power remains weak.

Table-2
Maximum value of external quantum efficiency according to the front external reflection

Front reflectance R (%)	EQE		
	Max value (%)	Incident wavelength (μm)	Incident energy (eV)
0	99.29	0.71	1.75
20	79.43	0.71	1.75
40	59.57	0.70-0.71	1.75-1.77
60	39.71	0.70-0.72	1.72-1.77
80	19.86	0.69-0.72	1.72-1.80

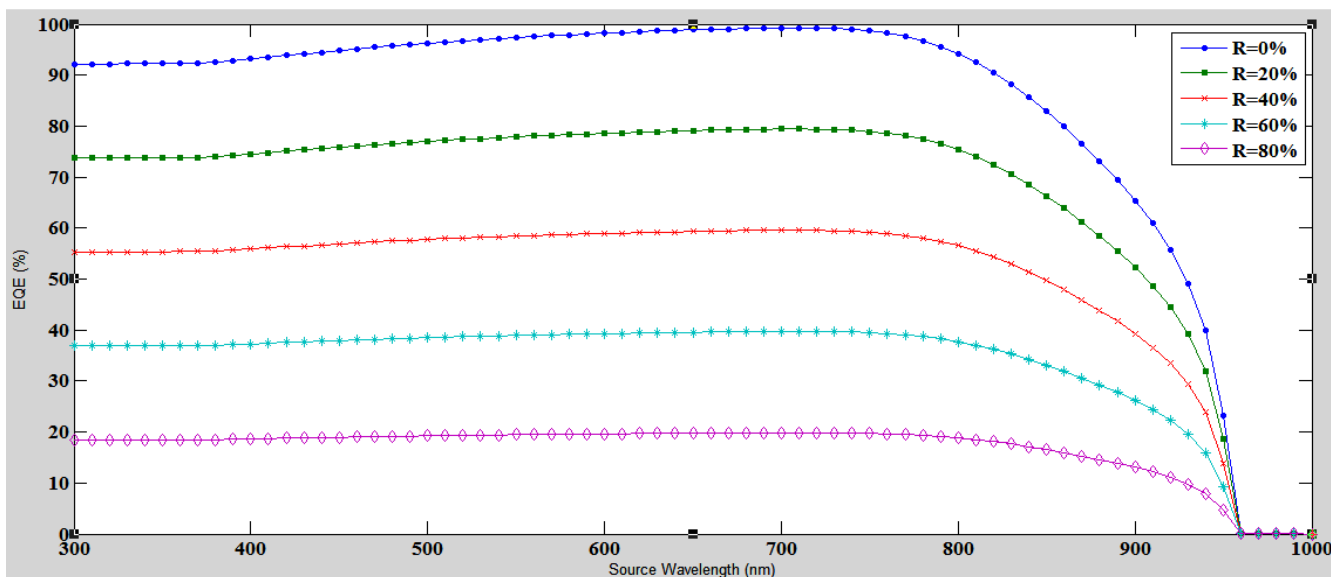


Figure-6
Variation of the quantum efficiency according to the front external reflection

Conclusion

We undertook a study on the consequences of the front external reflection on the electric parameters of the Cu(In, Ga)Se₂ thin film solar cell. We note that with the use of an "ideal" anti-reflecting layer, corresponding to a reflection of 0%, we can obtain an open circuit voltage of 0,8337V, a short circuit current density of 0.0325mA.cm⁻², a maximum power of cell of 0.0233mW and a maximum value of the external quantum efficiency of 99.29%. However these physical parameters are deeply affected by the front external reflection. Taking into account all the external factors which can slow down the absorption of the incidental light flux we use a maximum reflection coefficient of 80%. All the studied physical parameters decrease considerably. We find an open circuit voltage of 0,7923V, a short circuit current density of 0.0065mA.cm⁻², a maximum power of cell of 0.0045mW and a maximum value of the external quantum efficiency of 19.86%. We then note a fall in the open circuit voltage of 0.0414V, a fall in the short circuit current density of 0.026mA.cm⁻², a fall in the maximum power of the cell of 0.0188mW and a fall in the maximum value of the external quantum efficiency of 79.43%.

References

1. Ehemba A.K., Dieng M., Diallo D. and Sambou G. (2015). Influence of the donor doping density in CdS and Zn(O,S) buffer layers on the external quantum efficiency of Cu(In,Ga)Se₂ thin film solar cell. *International Journal of Engineering Trends and Technology*, 28(6), 280-286.
2. Soce M.M., Dieng M., Ehemba A.K., Diallo D. and Wade I. (2015). Influence of the doping of the absorber and the charged defects on the electrical performance of CIGS solar cells. *International Journal of Scientific and Research Publications*, 5(10), 1-6.
3. Diallo D., Dieng M. and Ehemba A.K. (2015). Modelling Defects Acceptors And Determination Of Electric Model From The Nyquist Plot And Bode In Thin Film CIGS. *International Journal of Scientific & Technology Research*, 4(12), 226-229.
4. Diagne O., Ehemba A.K., Diallo D., Wade I., SOCE M.M. and DIENG M. (2016). Effect of [Ga]/[In+Ga] Atomic Ratio on Electric Parameters of Cu(In,Ga)Se₂ Thin Film Solar Cells. *International Journal of Scientific Engineering and Technology*, 5(5), 252-255.
5. Ehemba A.K., Soce M.M., Wade I., Diallo D. and DIENG M. (2016). Influence of the use temperature on the Capacitance-Voltage measures and the external quantum efficiency of a Cu (In, Ga)Se₂ thin film solar cell. *Advances in Applied Science Research*, 7(3), 187-192.
6. Niane D., Ehemba A.K., Diallo D., Wade I. and Dieng M. (2016). the influence of temperature on the electric parameters of a solar cell based on Cu(In,Ga)Se₂. *International Journal of Scientific Engineering and Technology*, 5(5), 247-251.
7. Lee Y.J., Douglas S.R., David W.P., Bonnie B.M. and Julia W.P.H. (2008). ZnO Nanostructures as Efficient Antireflection Layers in Solar Cells. *Nano Lett.*, 8(5), 1501-1505.
8. Holman Z.C., De Wolf S. and Ballif C. (2013). Improving metal reflectors by suppressing surface plasmon polaritons: a priori calculation of the internal reflectance of a solar cell. *Science & Applications*, 106(2), doi:10.1038/lsa.2013.62.
9. Ehemba A.K. (2015). Determination de la longueur de diffusion des porteurs minoritaires par mesure de photocourant capacitance et détermination des paramètres électriques d'une cellule solaire à base de couche mince de CuInSe₂ électrodéposée sur substrat flexible de Kapton. Laboratoire des Semiconducteurs et d'Énergie Solaire, Université Cheikh Anta Diop, Dakar – Senegal.
10. Clugston D.A. and Basore P.A. (1997). PC1D version 5: 32-bit solar cell modeling on personal computers. Photovoltaic Specialists Conference, Conference Record of the Twenty-Sixth IEEE.
11. Belarbi M., Benyoucef A. and Benyoucef B. (2014). Simulation of the solar cells with PC1D, application to cells based on Silicon. *Advanced Energy: An International Journal (AEIJ)*, 1(3).
12. Salmi T., Bouzguenda M., Gastli A. and Masmoudi A. (2012). MATLAB/Simulink Based Modeling of Photovoltaic Cell. *International Journal of Renewable Energy Research*, 2(2), 213-218.
13. Mohammed. S. Sheik (2011). Modeling and Simulation of Photovoltaic module using MATLAB/Simulink. *International Journal of Chemical and Environmental Engineering*, 2(5), 350-355.